Intracardiac Vortex Dynamics by High-Frame-Rate Doppler Vortography—*In Vivo* Comparison With Vector Flow Mapping and 4-D Flow MRI

Julia Faurie, Mathilde Baudet, Kondo Claude Assi, Dominique Auger, Guillaume Gilbert, François Tournoux, and Damien Garcia

***Abstract*— Recent studies have suggested that intracardiac vortex flow imaging could be of clinical interest to early diagnose the diastolic heart function. Doppler vortography has been introduced as a simple color Doppler method to detect and quantify intraventricular vortices. This method is able to locate a vortex core based on the recognition of an antisymmetric pattern in the Doppler velocity field. Because the heart is a fast-moving organ, high frame rates are needed to decipher the whole blood vortex dynamics during diastole. In this paper, we adapted the vortography method to high-frame-rate echocardiography using circular waves. Time-resolved Doppler vortography was first validated in vitro in an ideal forced vortex. We observed a strong correlation between the core vorticity determined by high-frame-rate vortography and the ground-truth vorticity. Vortography was also tested *in vivo* in ten healthy volunteers using high-frame-rate duplex ultrasonography. The main vortex that forms during left ventricular filling was tracked during two–three successive cardiac cycles, and its core vorticity was determined at a sampling rate up to 80 duplex images per heartbeat. Three echocardiographic apical views were evaluated. Vortography-derived vorticities were compared with those returned by the 2-D vector flow mapping approach. Comparison with 4-D flow magnetic resonance imaging was also performed in four of the ten volunteers. Strong intermethod agreements were observed when determining the peak vorticity during early filling. It is concluded that high-frame-rate Doppler vortography can accurately investigate the diastolic vortex dynamics.**

***Index Terms*— Doppler vortography, high-frame-rate color Doppler, ultrafast ultrasound, vortex flow imaging.**

Manuscript received August 16, 2016; accepted November 22, 2016. Date of publication November 29, 2016; date of current version February 1, 2017. The work of D. Garcia was supported in part by the Canadian Institutes of Health Research under Grant MOP-106465, in part by the Fonds de Recherche du Québec - Nature et Technologies under Grant 2016-PR-189822, and in part by the Quebec Bio-Imaging Network under Grant 5886. The work of M. Baudet was supported by the French Federation of Cardiology. The work of D. Auger was supported by the Quebec Bio-Imaging Network under Grant 5886. The work of F. Tournoux was supported by the Fonds de recherche du Québec - Santé through a research scholarship award.

J. Faurie and K. C. Assi are with the Research Unit of Biomechanics and Imaging in Cardiology, Research Center of the University of Montreal Hospital, Montreal, QC H2X 0A9, Canada.

M. Baudet, D. Auger, and F. Tournoux are with the Echocardiographic Laboratory, University of Montreal Hospital, QC H2W 1T8, Canada.

G. Gilbert is with MR Clinical Science, Philips Healthcare Canada, Markham, ON L6C 2S3, Canada, and also with the Department of Radiology, Radio-Oncology and Nuclear Medicine, University of Montreal, QC H3T 1J4, Canada.

D. Garcia is with the Research Unit of Biomechanics and Imaging in Cardiology, Research Center of the University of Montreal Hospital, QC H2X 0A9, Canada, and also with the Department of Radiology, Radio-Oncology and Nuclear Medicine, University of Montreal, QC, Canada (e-mail: damien.garcia@crchum.qc.ca; garcia.damien@gmail.com).

Digital Object Identifier 10.1109/TUFFC.2016.2632707

I. Introduction

THE pattern of the intracardiac blood filling is strongly dependent on the myocardial shape. The eccentric position of the mitral valve relative to the cardiac chamber, as well as its structure, forces the left ventricular inflow to create a vortex ring that becomes elongated at end-diastole [1]. In a normal heart, the posterior cross section of the vortex ring quickly reaches the free wall, while the anterior cross section can attain the center of the intraventricular cavity. In this paper, we refer to the latter cross section as the *main diastolic vortex* when working on a 2-D plane of interest. This main vortex, by rotating in the natural flow direction, redirects blood momentum toward the left ventricular outflow tract and has been claimed to facilitate flow transit during ejection [2], [3]. When the filling of the left ventricle is impaired (diastolic dysfunction), a modification of the blood flow pattern can be observed, with a significant impact on the vortices [4]–[6]. The strength of a vortex in the left ventricle has been described in terms of various scalars, including circulation, vorticity, or kinetic energy [3]. Other vortex properties such as its shape [7], direction of rotation [8], and formation time [9], have also been shown to be of clinical interest. No clinical consensus has yet been reached on the vortical parameters that must be measured due to the recency and technical limitations of intracardiac vortex imaging. However, it is becoming indisputable that vortex flow properties can be used as quantitative clinical indices to provide an overview of the left ventricular filling [6], [10]. According to the recent clinical literature, it is expected that vortex flow imaging could lead to early diagnosis of the left ventricular diastolic dysfunction [11]. Most of the abovementioned vortex indices need planar or volumetric velocity vector components to be computed. Doppler vortography has been recently proposed to overcome this clinical limitation [12] by retrieving the core vorticity of a vortex from 2-D color Doppler fields only. In comparison with the vectorial imaging approaches, Doppler vortography is a simplified echocardiographic method based on color Doppler imaging, as clarified at the end of this section.

The intracardiac blood flow can be quantified noninvasively with magnetic resonance imaging (MRI), which can return 3-D velocity vectors [13]. However, due to the low frame rate, electrocardiogram (ECG)-gated multibeat acquisition and retrospective temporal registration are required to recover

the blood flow dynamics at a sufficient temporal resolution. Velocity encoding MRI is thus not used clinically because of its low cost-effectiveness. More clinically compatible noninvasive methods are based on ultrasound and can build a 2-D velocity field within an intraventricular blood flow. Vector flow imaging by ultrasound is often called echographic particle image velocimetry (*echo-PIV*) when gas-filled microbubbles are perfused to enhance the intensity of the blood signal [14], [15]. Ultrasound vector flow images can also be acquired without contrast agent by tracking the speckles emerging from the red blood cells [16]. This approach requires temporal high-pass filtering to remove the high-amplitude unwanted echoes (clutter), mostly generated by the surrounding tissues [17]. Contrast-enhanced echo-PIV is used in clinical research to analyze the dynamics of the vortices that form in the left ventricle [15], [18]. Its main clinical limitation is the intravenous administration of microbubbles. This procedure is highly time- and staff-consuming. *Vector flow mapping* (VFM) is another technique for vector flow imaging in the left ventricle. It is based on the postprocessing of color Doppler images [19], [20] and has been integrated in Hitachi ultrasound scanners [21]. This method assumes that the intraventricular flow is nearly 2-D in the standard echocardiographic long-axis views, so that the cross-beam velocity components can be estimated by minimizing the velocity divergence when appropriate wall conditions are used [19].

A technical limitation of the abovementioned techniques is the low frame rate with the current clinical scanners. Line-by-line sequential transmits limit cardiac B-mode imaging at $<$100 frames/s. The width and depth of the scan area must be thus reduced to obtain the conditions for an optimal speckle tracking (200 frames/s) [4]. VFM is also limited by a low frame rate. Since wall boundary conditions are necessary, it requires a large scan sector that encloses the left ventricular myocardium. This may reduce the frame rate to $<$15 frames/heartbeat with a conventional color Doppler sequence. Several consecutive heart cycles must be thus registered to obtain a comprehensive examination of the intracardiac flow, which can make VFM challenging in patients with cardiac arrhythmias and/or breath-holding difficulty. Recent technical advances in digital beamforming can speed up the frame rates of cardiac images up to 5–10 times [22], which can thus solve this frame rate dilemma. With regard to intracardiac vector flow imaging at high frame rates, promising results have been recently reported by Fadnes *et al*. [17] in neonate hearts with a linear array. Takahashi *et al*. [23] also illustrated the potential feasibility of blood speckle tracking in an adult left ventricle using diverging waves emitted by a phased array.

In this paper, we developed high-frame-rate Doppler vortography to recover the vorticity waveform of the main left ventricular vortex at a high temporal resolution. As described in [12], Doppler vortography is a quantitative ultrasound tool that uses the color Doppler images without the need of constructing vector fields. It is based on the centrosymmetric properties of the vortices, which produce an antisymmetric imprint in the Doppler data around the vortex cores [12], [24]. Doppler vortography quantifies the vortex strength by deriving an index called *blood vortex signature* (BVS), which allows the location of the vortex core and the computation of its vorticity. This innovative approach was first tested with conventional color Doppler imaging [12]. In the present work, we adapted Doppler vortography to high-frame-rate ultrasound (or "ultrafast ultrasound") with circular waves to get time-resolved Doppler vortography. Doppler vortography was incorporated in a duplex (B-mode + Doppler) imaging mode. High-frame-rate Doppler vortography was tested both *in vitro* and *in vivo*. Comparisons with high-frame-rate Doppler VFM and 4-D flow MRI were carried out.

II. Methods

Doppler vortography was generated using successive B-mode/Doppler sequences. We used diverging waves to obtain a suitable temporal resolution, as in our previous *in vivo* studies [25], [26]. High-frame-rate Doppler vortography was first tested in an ideal forced vortex simulated by a rotating disk. *In vivo* experiments were then carried out in ten volunteers to explore the feasibility and robustness of the proposed method in clinically realistic scenarios. Several echocardiographic long-axis views were analyzed and the intraventricular vorticities derived by Doppler vortography were compared with those obtained by: 1) VFM, using the Doppler technique developed in [19]; and 2) 4-D flow MRI [13]. The vortex dynamics was also examined in contrast with the E and A waves of the mitral inflow (i.e., early and late filling) returned by pulsed-wave Doppler with a clinical scanner.

A. High-Frame-Rate Duplex Imaging

We carried out the *in vitro* and *in vivo* experiments with a Verasonics research scanner (V-1-128, Verasonics Inc., Redmond, WA). The full aperture of a 2.5-MHz phased-array transducer (ATL P4-2, 64 elements, pitch = 0.32 mm) was used to transmit nontilted 60°-wide diverging circular wavefronts. With this configuration, the point source was located at a virtual position 1.75 cm behind the transducer (see (1) in [26]). Quadrature I/Q signals were acquired at a sampling rate of 10 MHz. No apodization was introduced in transmission or reception. The I/Q signals were migrated (synthetically focused) using a delay-and-sum. A 60°-wide sector scan composed of 256 radial scanlines was reconstructed during migration, at a radial sampling of 1 wavelength. A duplex sequence was implemented to get B-mode and Doppler images successively. B-mode images were generated by coherently compounding 16 frames obtained from the 60°-wide steered circular wavefronts. The tilt angles were linearly spaced between $-25°$ and $+25°$, and ordered in a triangle sequence. A motion-compensation technique was integrated in the coherent compounding process to obtain high-quality B-mode images (i.e., no destructive interference due to motion) [26]. The triangle sequence of the tilt angles helps to minimize the adverse effects of the receipt sidelobes, as explained thoroughly in [26]. Doppler images were generated from a packet of unsteered 60°-wide transmits (no coherent compounding, packet size from 16 to 32, depending on the heart rate of the subject) using an I/Q autocorrelator [27]. The I/Q signals were clutter-filtered globally by

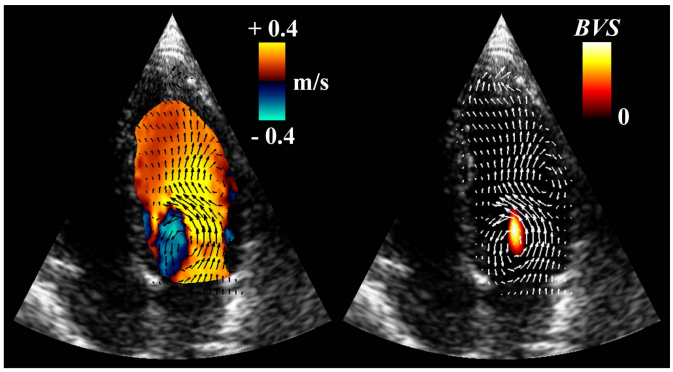

Fig. 1. Left: Doppler field in the left ventricle (red/blue color map) with the corresponding velocity field given by the VFM (black arrows). Right: Corresponding map of the BVS for the same high-frame-rate sequence, as returned by Doppler vortography. The local extremum of the BVS returns the location of the vortex core. For comparison, the overlaid white arrows represent the VFM map of the left panel.

converting each ensemble of the observations, i.e., each packet, into principal components (principal component analysis) [28] and discarding the 30% eigenvectors of highest energy. This threshold was set heuristically. Pulses of 2 (or 8) wavelengths were transmitted for the B-(or Doppler) mode at a pulse repetition frequency >3000 Hz to get >60 duplex (B-mode + Doppler) images per heartbeat. Acquisition time was set to 2 or 3 s *in vivo* to obtain at least two cardiac cycles.

B. Tracking of the Main Vortex by Doppler Vortography

Doppler vortography is a recent technique developed by our group to identify vortices in a Doppler field and locate their core centers. It is fully described in [12]. As explained in the introduction, Doppler vortography is based on the recognition of the Doppler field antisymmetric patterns created by a vortex flow: when scanning a vortical flow, the Doppler field exhibits a scan line of zeroes crossing the vortex center surrounded by two extrema of opposite signs. Mathematically speaking, flipping left to right a small kernel centered on the vortical core mostly modifies its sign only. In Doppler vortography, a sliding-block processing is used to detect these specific signatures and returns a scalar BVS map. The BVS is a nonphysical index that allows one to point out a vortex. The local extrema of the BVS correspond to the vortex cores (Fig. 1). Assuming a centrosymmetric core swirling, the core vorticity (i.e., the curl of the blood velocity at the vortex center) can be then deduced from the local Doppler velocities V_D: $\omega_c = (2/r_c)(\partial V_D/\partial\theta)$, at (r_c, θ_c) [12, eq. (7)], where r_c and θ_c stand for the radial and angular coordinates of the vortex center (where BVS is extremal). By retrieving the value of the core vorticity for each Doppler field of the high-frame-rate sequence, the dynamics of the main vortex can be derived over time. The vortography method is based on a sliding-block operation. It has been shown [12] that the size of the blocks has a minor effect on the core vorticity estimates. In this paper, the block size was set at 1/5 the size of the Doppler image before postscanning.

C. In Vitro Studies

High-frame-rate Doppler vortography was tested *in vitro* on a tissue-mimicking spinning disk (diameter 2 and 3 cm) to simulate an ideal forced vortex (rigid rotation). This disk was immersed in a water tank and mounted on a step motor to control its rotational speed. Its weight composition was agar 3%, Sigmacell cellulose powder 3%, and water. The angular velocity Ω ranged from 2π to 26π rad/s (with an increment of 2 rad/s), which gave a core vorticity range of [12 s^{-1} – 163 s^{-1}] compatible with that observed within an adult heart. The size and velocity values were chosen to be consistent with the clinical observations [18], [19]. The disk was scanned by a 2.5 MHz phased array using the diverging beam sequence described earlier (one packet of 32 unsteered transmits). The measurements were repeated ten times after switching OFF the system between each experiment to minimize the statistical dependence between the successive data sets. A total of 260 measures were obtained (2 diameters × 13 speeds × 10 times = 260). The core vorticities determined by Doppler vortography was compared with the ground-truth vorticities given by the angular velocities of the disk: $\omega_{\text{ref}} = 2\ \Omega$. To check whether the position of the probe could introduce a significant bias in the vortography-derived core vorticities, we also tested four insonation (azimuthal) plane angles with respect to the disk axis (0°, 10°, 15°, and 20°). In clinical practice, the inclination of the probe relative to the left ventricle axis varies little from one patient to another, since it is essentially described by specific anatomic references.

D. In Vivo Studies

High-frame-rate Doppler vortography was applied *in vivo* in ten volunteers without known cardiac disease (23–42 y/o). Heart rate ranged from 48 to 120 bpm. The transducer was placed right upon the cardiac apex to acquire three successive apical views, namely, the three-, four- and five-chamber views (Fig. 2). The core vorticities of the main vortex derived from the three views were compared against each other. To obtain a ground-truth waveform of the diastolic flow dynamics, the mitral inflow velocity was measured by pulsed-wave Doppler with a portable clinical scanner (Vivid q, GE Healthcare). ECGs were simultaneously recorded by the Vivid q system. For visual purposes (as in Fig. 5), the diastolic onsets of the nonsimultaneous data issued from the Verasonics and Vivid q scanners were synchronized by matching the mitral valve opening (visible in the B-mode, Verasonics) with the end of the ECG T-wave (Vivid q). The protocol was approved by the human ethical review committee of the CRCHUM.

E. High-Frame-Rate Vector Flow Mapping

High-frame-rate Doppler vortography was compared against VFM [19], as in [12]. VFM is a technique for intraventricular vector flow imaging based on the postprocessing of color Doppler images [19] (Fig. 1). In comparison with Doppler vortography, which directly targets the vortical flow patterns, this method returns a full 2-D vector field and does not necessarily yield axisymmetric vortices. In this

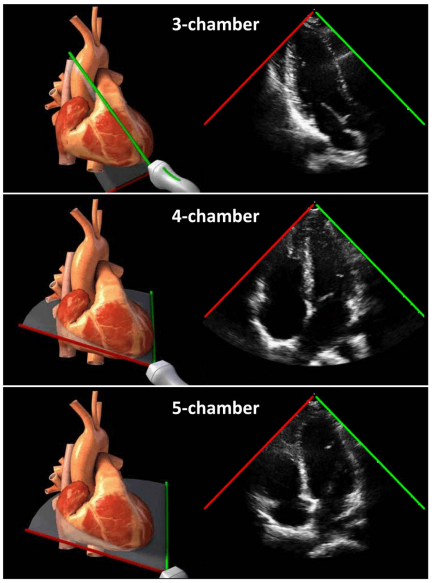

Fig. 2. Three standard echocardiographic apical views. In the present study, the 3-, 4P- and 5-chamber views were all analyzed by high-frame Doppler vortography. Images reproduced with permission from http://pie.med.utoronto.ca/tte.

paper, the *in vivo* Doppler data obtained from the Verasonics sequences, and used for Doppler vortography, were also exploited to generate high-frame-rate VFM. These data were postprocessed using a reformulation of that initially reported in [19]. The VFM method was written as a regularized least-squares problem, where a regularization term was inspired by the constraint of a 2-D null-divergence flow pattern. A finite difference discretization of the derivative operators in the cost function was adopted. The regularization parameters were determined automatically by analyzing the L-hypersurface, a generalization of the L-curve [29]. The reformulated approach for VFM will be the subject of a forthcoming paper, which will include the numerical details. The vorticity maps were derived from the 2-D velocity vector fields using the eight-point method [30]. The core vorticity was defined as the maximal vorticity value of the main vortex. The core vorticities estimated by Doppler vortography were compared against those derived by VFM in the ten volunteers. Only the four-chamber view was analyzed for this test since it generally provided the best view of the vortex, and the position of the mitral valve created less clutter on this cross section.

F. 4-D Flow MRI

The intraventricular blood velocities were finally measured by 4-D flow MRI in four of the ten volunteers. Four-dimensional flow MRI refers to volumetric MRI data acquired in a time-resolved manner with velocity encoding in all the three spatial directions [31]. A Philips Achieva TX 3T MRI scanner was used to collect the volumetric three-component velocities in the left ventricle. Velocity encoding was achieved in all the three dimensions at a sampling rate of 25 to 30 frames per cardiac cycle, using a respiratory navigator-gated and retrospectively cardiac-gated sequence with a nominal isotropic spatial resolution of 3 mm. After completion

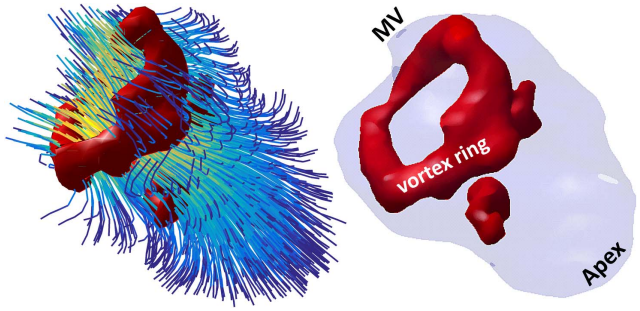

Fig. 3. Image of the vortex ring forming in the left ventricle during early filling obtained by 4-D flow MRI. MV—mitral valve. The red isosurfaces delimit the regions of strong vorticity. The streamlines of the left panel show the flow direction in the left ventricular cavity.

of the acquisition, the data were registered temporally to reconstruct a complete cardiac cycle. To retrieve the vorticity within the blood flow volume, we first proceeded to a manual segmentation of the left ventricular endocardium under the supervision of a cardiologist. The vortical volume of interest was then detected using the Q-criterion [32] (Fig. 3) and the magnitude of the vorticity vectors was computed inside those defined regions. The core vorticity curves obtained by 4-D flow MRI were compared with those returned by the Doppler vortography technique. The MRI- and vortography-derived vorticity curves were first normalized in space and time to take into account the following:

1) the spatial averaging resulting from the relatively low nominal spatial resolution of the 4D-flow MRI sequence;
2) the temporal averaging resulting from the collection of data over multiple cardiac cycles (both leading to an underestimation of MRI-derived vorticity magnitude);
3) the significant decrease in heartbeat occurring in the MRI scanner due to the extended resting conditions.

G. Statistical Analyses

The vortography-derived and ground-truth *in vitro* vorticities were compared using a linear regression and a Bland–Altman plot. Two-way mixed single-measures intraclass correlation coefficients (ICC) and their 95% confidence intervals were calculated to analyze the intermethod reliability [33] when estimating the *in vivo* core vorticities. The peak vorticities determined in the ten volunteers during early and late filling (E-vorticity and A-vorticity) as well as the peak-to-peak delays (E-A) were compared as follows: 1) Doppler vortography: comparison between the three echocardiographic views (3, 4, and 5-chamber) and 2) Doppler vortography (4-chamber view) vs. VFM (4-chamber view). The peak-to-peak delays measured by Doppler vortography were also compared with those obtained by pulsed-wave Doppler (delay between the E-wave and A-wave). A second series of ICC analyses was also carried out: ICC coefficients were computed per subject using the complete vorticity ensemble acquired during one cardiac cycle. For each subject, the complete core-vorticity time series were compared as follows: 1) Doppler vortography: comparison between the three echocardiographic views (3, 4, and 5-chamber, 10 subjects); 2) Doppler

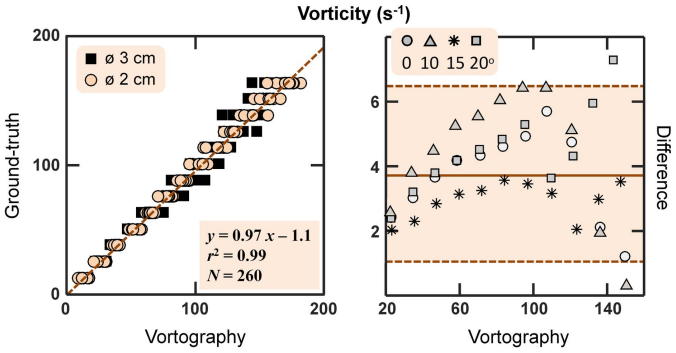

Fig. 4. Left: Linear regression between the ground-truth and vortography-derived vorticities (*in vitro* study). Right: Absolute difference between the ground-truth and vortography-derived vorticities (Bland–Altman plot) for the four different azimuthal angles.

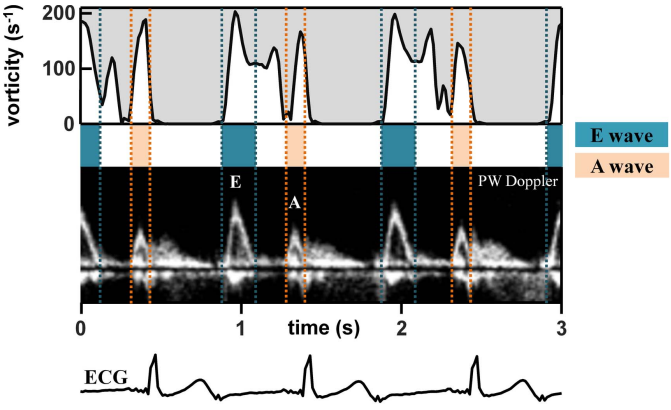

Fig. 5. Core vorticity of the main vortex estimated by high-frame-rate Doppler vortography. The vortex dynamics is compared with the mitral inflow measured by pulsed-wave Doppler with a clinical portable scanner.

vortography versus VFM (ten subjects) and 3) Doppler vortography versus 4-D flow MRI (4 subjects). For these individual analyses, the vorticity time series were linearly interpolated (with respect to the shortest series) to allow timewise comparisons. The ICC were calculated in terms of absolute agreement (ICC-A) since systematic differences between the different methods were relevant. However, ICC in terms of consistency (ICC-C, i.e., systematic differences were irrelevant) were reported for the comparison with the MRI-derived vorticities since normalization was required, as explained earlier.

III. Results

A. In Vitro Vorticities in the Spinning Disk

Strong concordance and correlation ($r^2 = 0.99$, $y = 0.97\ x - 1.1$, $N = 260$, Fig. 4, left) were observed between the vortography-derived vorticities and the ground-truth vorticities, with both the 2- and 3-cm disks. The insonation angle had little effect on the core vorticity estimates (Fig. 4, right). The mean error was $< 8\ s^{-1}$ for each angle. These *in vitro* results show that the core vorticities derived by Doppler vortography based on circular waves are robust to the ultrasound beam inclination.

B. In Vivo Time-Resolved Vorticities by Doppler Vortography

The main vortices of the ten volunteers were successfully tracked during two to three cardiac cycles by high-frame-rate Doppler vortography. A number of 60–80 high-quality Duplex images per heartbeat were obtained, allowing an effective monitoring of the different cardiac phases (early diastole, diastasis, late diastole, and systole). Biphasic (triphasic in some cases) dynamic vortical patterns were observed during diastole (see an example in Fig. 5): a first peak appearing during early filling (ventricular relaxation) and a last one in late filling (atrial contraction). The vortex persisted during isovolumic contraction then vanished during ejection. The peak vorticities measured by Doppler vortography were $159 \pm 36\ s^{-1}$ during early filling (ventricular relaxation), and $108 \pm 28\ s^{-1}$ in late filling (atrial contraction). Fig. 5 shows how the core vorticity of the main intraventricular vortex varied temporally through diastole. The first and last peaks were synchronized with the E and A waves of the mitral inflow. In this example, an intermediate vorticity peak appeared during diastasis, likely related to the L-wave observable in healthy subjects with relatively low heart rates [34].

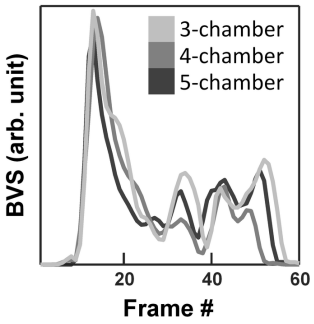

Fig. 6. BVS waveform during diastole in one subject: comparison between the three apical echocardiographic views.

C. Comparison Between the three Echocardiographic Views

Fig. 6 shows the three curves of the diastolic BVS extrema—corresponding to the three different echo views—for the subject with the best three views. Similar dynamics and amplitude of BVS were obtained. Note that the BVS is a numerical imprint of vortices and has no actual physical meaning. The comparison between the core vorticities (in s^{-1}) in the same subject is illustrated in Fig. 7. Although the Doppler measurements were not simultaneous, the vortex measures obtained from the three apical echocardiographic views were comparable for the E-vorticity and the E-A delay (ICC-A = 0.78 and 0.95, respectively: excellent intermethod reliability, Fig. 8). The intermethod reliability of the A-vorticity measurement, however, was only fair (ICC-A = 0.5, Fig. 8); this denotes a significant dependence upon the echo view, likely because the vortex ring is no longer toroidal in late diastole [1], [9]. The individual timewise intermethod agreements were good to excellent (ICC-A between 0.68 and 0.9) in seven subjects and fair (ICC-A<0.59) in three subjects (Fig. 9).

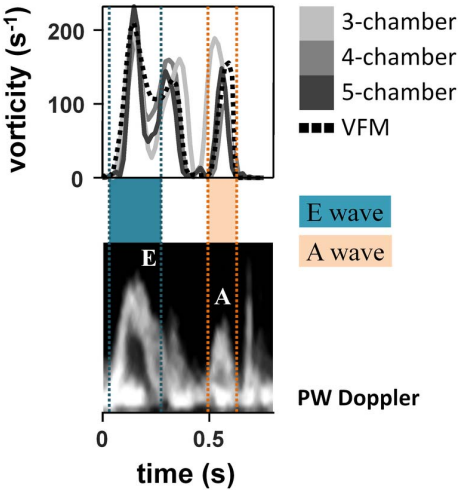

Fig. 7. Core vorticity of the main vortex estimated by high-frame-rate Doppler vortography: comparison between the three apical echocardiographic views and with VFM. The vortex dynamics is compared with the mitral inflow measured by pulsed-wave Doppler with a clinical portable scanner.

	E-vorticity	A-vorticity	E-A
3 ch / 4 ch / 5 ch	0.78 [0.51 - 0.93]	0.5 [0.12 - 0.82]	0.95 [0.87 - 0.99]
4 ch / VFM	0.89 [0.6 - 0.97]	0.7 [0 - 0.93]	0.99 [0.95 - 1]
4 ch / PW			0.9 [0.68 - 0.97]

Poor	Fair	Good	Excellent
0 – 0.39	0.4 – 0.59	0.6 – 0.74	0.75 – 1

Fig. 8. Intermethod agreement measured by the ICC (model: two-way mixed; type: absolute agreement; single measures). 3 ch/4 ch/5 ch—Doppler vortography using the 3-, 4- or 5-chamber view. VFM—with the 4-chamber view. PW—mitral inflow by pulsed-wave Doppler. The 95% confidence intervals are in square brackets.

Although a larger sample size would be necessary to draw a firm conclusion, the *in vivo* study tends to show that the three apical echocardiographic views can be used interchangeably, in particular for the E-vorticity.

D. Comparison With Vector Flow Mapping and PW Doppler

Fig. 7 also shows that the vortography method led to similar results as the VFM method. The reliability between the two methods was rated as excellent for the E-vorticity and the E-A delay (ICC-A = 0.89 and 0.99, Fig. 8). This is concordant with our previous findings (vortography- versus VFM-derived vorticities, $r^2 = 0.89$) obtained in 55 Doppler frames of 19 patients with conventional Doppler echocardiography [12]. The intermethod reliability of the A-vorticity measurement, however, was weaker (good agreement, ICC-A = 0.7, Fig. 8). The wide 95% confidence interval [(0 – 0.93)] denoted a large variance due to the presence of outliers. This might be explained in part by the inherent simplification of Doppler vortography, which assumes nearly circular vortices. Finally, the dynamic reliability (quantified by the E-A delay) between Doppler vortography and pulsed-wave Doppler was excellent (ICC-A = 0.9, Fig. 8): the vortex dynamics was expectedly related to the mitral inflow pattern.

	3 – 4 – 5 ch	4 ch / VFM	4 ch / MRI
1	0.8 [0.69 – 0.87]	0.9 [0.89 – 0.94]	0.88 [0.74 – 0.94]
2	0.58 [0.43 – 0.7]	0.51 [0.06 – 0.75]	0.76 [0.55 – 0.88]
3	0.9 [0.83 – 0.94]	0.78 [0.21 – 0.92]	0.79 [0.58 – 0.9]
4	0.73 [0.6 – 0.83]	0.89 [0.79– 0.94]	0.69 [0.3 – 0.88]
5	0.72 [0.6 – 0.8]	0.89 [0. 83– 0.93]	
6	0.51 [0.29 – 0.68]	0.91 [0.85 – 0.95]	
7	0.7 [0.56 – 0.81]	0.52 [0. 28– 0.71]	
8	0.74 [0.6 – 0.85]	0.88 [0.78 – 0.93]	
9	0.56 [0.38 – 0.71]	0.63 [0 – 0.85]	
10	0.68 [0. 43– 0.82]	0.87 [0.79 – 0.92]	

Poor	Fair	Good	Excellent
0 – 0.39	0.4 – 0.59	0.6 – 0.74	0.75 – 1

Fig. 9. Intermethod agreement measured individually by the ICC, for each of the 10 subjects and for the complete vorticity ensemble acquired during one cardiac cycle (only 4 subjects with MRI). ICC model: two-way mixed. ICC type: absolute agreement (Doppler) or consistency (MRI), single measures. 3 – 4 – 5 ch—Doppler vortography using the 3-, 4- or 5-chamber view. VFM—with the 4-chamber view. MRI—4-D flow. The 95% confidence intervals are in square brackets.

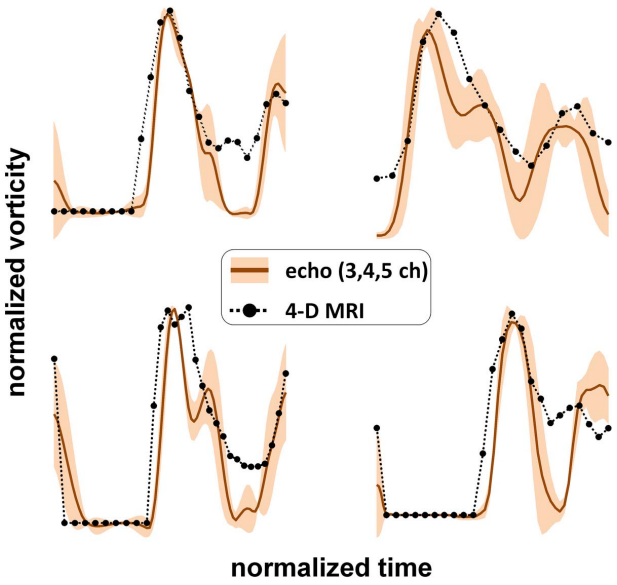

Fig. 10. Normalized core vorticity of the main vortex during a cardiac cycle: high-frame-rate Doppler vortography (3, 4, and 5-chanber views) versus ECG-gated 4-D flow MRI. The solid line represents the average of the three echocardiographic views; the shaded areas represent the range.

E. Comparison With 4-D Flow MRI

Despite the low temporal resolution of 4-D flow MRI, the two vorticity peaks related to the E and A waves were observable. When the core vorticities were normalized both in time and magnitude, the vortex dynamics obtained by Doppler vortography and 4-D flow MRI were alike (Fig. 10) in the four subjects. Good to excellent individual MRI-versus-vortography agreements were observed (ICC-C between 0.69 and 0.88), denoting a similar biphasic

vortex dynamics. These results tend to show that the absence of the third dimension in Doppler vortography is not critical to retrieve the vorticity of the main vortex in the left ventricle.

IV. Discussion

Doppler vortography detects and quantifies the intraventricular vortices by analyzing the patterns of the Doppler field [12], a concept first initiated in weather Doppler radar for the detection of tornadoes [24]. This paper introduced high-frame-rate Doppler vortography. A frame rate $\sim$5 times higher than conventional ultrasound imaging was obtained for duplex imaging (color Doppler interleaved with B-mode). Color Doppler was obtained using packets of unsteered circular waves [25], while high-quality B-mode images were produced by coherent compounding with integrated motion compensation [26]. Up to 80 duplex images per cardiac cycle were obtained; high-frame-rate Doppler vortography can thus investigate the diastolic vortex dynamics in a single heartbeat. As demonstrated by the *in vitro* results, Doppler vortography is very accurate for an ideal planar vortex and is little sensitive to any inclination of the insonation plane. The intraventricular vortex in the human heart, however, is 3-D, as illustrated by the vortex ring detected by 4-D flow MRI ([1] and Fig. 3). As long as this vortex ring is nearly toroidal (doughnut shaped) and perpendicular to the probe axis, the assumptions in Doppler vortography are acceptable, and the method is expected to be roughly independent of the selected apical echocardiographic view (Fig. 2). This was noticeable during early filling (E-vorticity) in which the intermethod reliability was excellent (Fig. 8). During late filling (A-vorticity), however, the intermethod agreement was weaker (fair to good). The A-vortex ring is indeed known to be elongated in normal subjects [1], resulting in different vorticity projections onto the long-axis echocardiographic planes; this could explained the smaller intraclass coefficients reported in late diastole. These results suggest that any one long-axis view is suitable for investigation of the intraventricular main E-vortex; however, the echographic views are likely not interchangeable for the measurement of the A-vorticity. It must be noticed that one cannot assure that an accurate estimation of the E-vorticity by Doppler vortography is always achievable. Our toroidal assumption may fail in some cardiomyopathies with disturbed intracardiac flows, such as aortic insufficiency or asymmetric septal hypertrophy, to name a few. A larger cohort would be required to confirm our conclusions since only ten healthy volunteers were included in this paper.

A. Using 1-D Velocity Components for Vortex Quantification

In comparison with the commonest clinical methods for vortex quantification mentioned in Section I (echo-PIV, cardiac magnetic resonance, VFM), Doppler vortography uses only one velocity component: the component parallel to the ultrasound beam provided by color Doppler. Because it requires straightforward measurements and postprocessing, two substantial advantages of Doppler vortography are its clinical compliance and usability. However, the problem of deciphering a 3-D flow with a single component is ill-posed, unless more or less realistic premises are formulated. Doppler vortography assumes that: 1) the vortex is large enough to generate a local and detectable centrosymmetric pattern in the Doppler field and 2) the vortex core is almost circular in the echo plane to allow the estimation of its vorticity. The lateral angular resolution of color Doppler is sufficient to meet the first condition. It was also found in this paper that the second condition is fulfilled in early diastole (E-vortex). This second prerequisite, however, seems to be lacking during atrial contraction (A-vortex), as highlighted by the relatively low ICC values. This is not an unexpected result as previous MRI studies showed that the vortex ring is relatively elongated during late filling [1]. In short, the 1-D vortography method is well adapted to the quantification of the main vortex during ventricular relaxation. We anticipate that vortex flow imaging by high-frame-rate Doppler vortography will be clinically relevant for better assessment of the diastolic function.

B. Toward 3-D Vortex Flow Imaging?

The advent of 3-D echo has significantly impacted the clinical management of cardiac diseases. In recent years, many clinical studies have investigated its value in cardiac diagnosis [35]. Clinicians now agree that 3-D echo imaging can be both complementary and supplementary to 2-D echo imaging. In the nature of things, with the recent advances in digital beamforming and postprocessing for ultrasound imaging, 3-D vortex flow imaging by echocardiography will most likely be available in the near future. Three recent *in vivo* studies are key indicators of this trend:

1) Three-dimensional ultrasound analyses of the intraventricular flow vortex were first carried out using multiplanar reconstructions of echo-PIV images obtained by biplane echocardiography [36].
2) Gomez *et al.* [37] derived volumetric three-component velocity vector imaging in the left ventricle by registering several linearly independent color Doppler volumes.
3) Provost *et al.* [38] introduced 3-D intracardiac Doppler imaging at a high volume rate.

Using proper fluid-dynamics models, Doppler vortography and VFM could be adapted to 3-D color flow imaging. Three-dimensional time-resolved vortex flow imaging (by color Doppler, speckle tracking, or multiview registration) will logically be of great interest for diastology in clinical research. Following the example of 3-D grayscale imaging, the relevance of 3-D vortex flow imaging in daily practice can however be curtailed due to limited ease-of-use and learnability. A major issue will be the flow visualization and how the substantial amount of volumetric flow data must be exploited in the clinic.

C. Limitations and Potential Improvements

High frame rates were obtained through transmits of diverging beams. Since acoustic pressure [and in turn, the signal-to-noise ratio (SNR)] decreases as beams become wider, this may tend to increase Doppler variance significantly. On the other hand, high-frame-rate imaging allows increasing the packet size and thus decreasing its variance. Since Doppler variance

is more sensitive to SNR than to the packet size [39], it is likely that the use of unfocused waves can negatively affect Doppler precision. Moreover, the I/Q Doppler data were not compound since the acoustic beams were unsteered (no coherent compounding), which is known to reduce image quality (lower contrast and spatial resolution) in comparison with focused beams. However, our previous study on ultrafast color Doppler [25] tends to demonstrate that accurate Doppler velocities can be obtained with wide unfocused beams transmitted by a cardiac phased array. The present study now shows that diverging wave imaging generates color-Doppler images with sufficient quality to track the main vortex and determine its vorticity with satisfactory accuracy. However, one of the main challenges with high-frame-rate Doppler vortography was clutter removal. The use of diverging waves made the clutter signals caused by the mitral leaflets spread over the width of the scan sector (we noticed that the four-chamber view was less prone to clutter). Although the principal component analysis removed a large part of the clutter, significant artifacts remained visible in some Doppler frames. Conveniently, as the vortex core was located downstream of the leaflet tips, the corresponding Doppler signals were slightly affected by clutter. The vortography method thus remained efficient, even with persistent clutter around the mitral valve. Clutter filtering could be notably improved using a local adaptive eigen-based technique with automatic selection of cutoff values. This approach is well adapted for microvascular flow [40]; whether it can improve intracardiac Doppler images with the high-frame-rate sequence proposed in the present study must be investigated. Finally, it is to be noted that we used a simple diffraction summation (delay-and-sum) to beamform the signals. A more advanced beamforming approach could help to mitigate the spread of the clutter signals. Other high-frame-rate sequences likely less sensitive to spread Doppler clutter could be also investigated, such as the multitransmit method [41]. The small sample size was another limitation of this study. Only ten healthy volunteers were scanned to test the clinical feasibility of high-frame-rate Doppler vortography. In future studies, the intra- and interobserver reproducibility will have to be evaluated in a larger cohort. Subjects with cardiac remodeling must also be included to cover a wider range of myocardium geometries.

V. Conclusion

High-frame-rate Doppler vortography was able to locate the core of the main intraventricular vortex and quantify its vorticity in a single heartbeat. The vortex dynamics were highly consistent with those determined by VFM and 4-D flow MRI. High-frame-rate Doppler vortography may offer new echographic insights into left ventricular diastolic function. This innovative technique uses Doppler, nothing more, and has the strong advantage to be fast and reproducible.

References

[1] M. S. M. Elbaz, E. E. Calkoen, J. J. M. Westenberg, B. P. F. Lelieveldt, A. A. W. Roest, and R. J. van der Geest, "Vortex flow during early and late left ventricular filling in normal subjects: Quantitative characterization using retrospectively-gated 4D flow cardiovascular magnetic resonance and three-dimensional vortex core analysis," *J. Cardiovascular Magn. Reson.*, vol. 16, p. 78, Sep. 2014.

[2] P. J. Kilner, G.-Z. Yang, A. J. Wilkes, R. H. Mohiaddin, D. N. Firmin, and M. H. Yacoub, "Asymmetric redirection of flow through the heart," *Nature*, vol. 404, no. 6779, pp. 759–761, Apr. 2000.

[3] J. Bermejo, P. Martínez-Legazpi, and J. C. del Álamo, "The clinical assessment of intraventricular flows," *Annu. Rev. Fluid Mech.*, vol. 47, no. 1, pp. 315–342, Jan. 2015.

[4] H. Abe *et al.*, "Contrast echocardiography for assessing left ventricular vortex strength in heart failure: A prospective cohort study," *Eur. Heart J.-Cardiovascular Imag.*, vol. 14, no. 11, pp. 1049–1060, 2013.

[5] J. Bermejo *et al.*, "Intraventricular vortex properties in nonischemic dilated cardiomyopathy," *Amer. J. Physiol.-Heart Circulatory Physiol.*, vol. 306, no. 5, pp. H718–H729, 2014.

[6] D. R. Muñoz *et al.*, "Left ventricular vortices as observed by vector flow mapping: Main determinants and their relation to left ventricular filling," *Echocardiography*, vol. 32, no. 1, pp. 96–105, Jan. 2015.

[7] S. Cimino *et al.*, "*In vivo* analysis of intraventricular fluid dynamics in healthy hearts," *Eur. J. Mech. B, Fluids*, vol. 35, pp. 40–46, Sep./Oct. 2012.

[8] G. Pedrizzetti, F. Domenichini, and G. Tonti, "On the left ventricular vortex reversal after mitral valve replacement," *Ann. Biomed. Eng.*, vol. 38, no. 3, pp. 769–773, Mar. 2010.

[9] A. Kheradvar, R. Assadi, A. Falahatpisheh, and P. P. Sengupta, "Assessment of transmitral vortex formation in patients with diastolic dysfunction," *J. Amer. Soc. Echocardiogr.*, vol. 25, no. 2, pp. 220–227, 2012.

[10] P. P. Sengupta *et al.*, "Emerging trends in CV flow visualization," *JACC Cardiovascular Imag.*, vol. 5, no. 3, pp. 305–316, 2012.

[11] G. Pedrizzetti, G. La Canna, O. Alfieri, and G. Tonti, "The vortex—An early predictor of cardiovascular outcome?" *Nature Rev. Cardiol.*, vol. 11, no. 9, pp. 545–553, Jun. 2014.

[12] F. Mehregan *et al.*, "Doppler vortography: A color Doppler approach to quantification of intraventricular blood flow vortices," *Ultrasound Med. Biol.*, vol. 40, no. 1, pp. 210–221, Jan. 2014.

[13] M. Markl, P. J. Kilner, and T. Ebbers, "Comprehensive 4D velocity mapping of the heart and great vessels by cardiovascular magnetic resonance," *J. Cardiovascular Magn. Reson.*, vol. 13, p. 7, Jan. 2011.

[14] H. B. Kim, J. R. Hertzberg, and R. Shandas, "Development and validation of echo PIV," *Experim. Fluids*, vol. 36, no. 3, pp. 455–462, Mar. 2004.

[15] A. Kheradvar *et al.*, "Echocardiographic particle image velocimetry: A novel technique for quantification of left ventricular blood vorticity pattern," *J. Amer. Soc. Echocardiogr.*, vol. 23, no. 1, pp. 86–94, Jan. 2010.

[16] G. E. Trahey, S. M. Hubbard, and O. T. von Ramm, "Angle independent ultrasonic blood flow detection by frame-to-frame correlation of B-mode images," *Ultrasonics*, vol. 26, no. 5, pp. 271–276, Sep. 1988.

[17] S. Fadnes, S. A. Nyrnes, H. Torp, and L. Lovstakken, "Shunt flow evaluation in congenital heart disease based on two-dimensional speckle tracking," *Ultrasound Med. Biol.*, vol. 40, no. 10, pp. 2379–2391, Oct. 2014.

[18] G.-R. Hong *et al.*, "Characterization and quantification of vortex flow in the human left ventricle by contrast echocardiography using vector particle image velocimetry," *JACC Cardiovascular Imag.*, vol. 1, no. 6, pp. 705–717, 2008.

[19] D. Garcia *et al.*, "Two-dimensional intraventricular flow mapping by digital processing conventional color-Doppler echocardiography images," *IEEE Trans. Med. Imag.*, vol. 29, no. 10, pp. 1701–1713, Oct. 2010.

[20] T. Uejima *et al.*, "A new echocardiographic method for identifying vortex flow in the left ventricle: Numerical validation," *Ultrasound Med. Biol.*, vol. 36, no. 5, pp. 772–788, May 2010.

[21] T. Tanaka *et al.*, "Intracardiac VFM technique using diagnostic ultrasound system," *Hitachi Rev.*, vol. 64, no. 8, pp. 489–492, 2015.

[22] M. Cikes, L. Tong, G. R. Sutherland, and J. D'hooge, "Ultrafast cardiac ultrasound imaging: Technical principles, applications, and clinical benefits," *JACC Cardiovascular Imag.*, vol. 7, no. 8, pp. 812–823, 2014.

[23] H. Takahashi, H. Hasegawa, and H. Kanai, "Echo speckle imaging of blood particles with high-frame-rate echocardiography," *Jpn. J. Appl. Phys.*, vol. 53, no. 7S, pp. 07KF08-1–07KF08-7, 2014.

[24] R. A. Brown, L. R. Lemon, and D. W. Burgess, "Tornado detection by pulsed Doppler radar," *Mon. Weather Rev.*, vol. 106, no. 1, pp. 29–38, 1978.

[25] D. Posada *et al.*, "Staggered multiple-PRF ultrafast color Doppler," *IEEE Trans. Med. Imag.*, vol. 35, no. 6, pp. 1510–1521, Jun. 2016.

[26] J. Porée, D. Posada, A. Hodzic, F. Tournoux, G. Cloutier, and D. Garcia, "High-frame-rate echocardiography using coherent compounding with Doppler-based motion-compensation," *IEEE Trans. Med. Imag.*, vol. 35, no. 7, pp. 1647–1657, Jul. 2016.
[27] T. Loupas, J. T. Powers, and R. W. Gill, "An axial velocity estimator for ultrasound blood flow imaging, based on a full evaluation of the Doppler equation by means of a two-dimensional autocorrelation approach," *IEEE Trans. Ultrason., Ferroelect., Freq. Control*, vol. 42, no. 4, pp. 672–688, Jul. 1995.
[28] S. Bjaerum, H. Torp, and K. Kristoffersen, "Clutter filters adapted to tissue motion in ultrasound color flow imaging," *IEEE Trans. Ultrason., Ferroelect., Freq. Control*, vol. 49, no. 6, pp. 693–704, Jun. 2002.
[29] M. Belge, M. E. Kilmer, and E. L. Miller, "Efficient determination of multiple regularization parameters in a generalized L-curve framework," *Inverse Problems*, vol. 18, no. 4, p. 1161, 2002.
[30] J. D. Luff, T. Drouillard, A. M. Rompage, M. A. Linne, and J. R. Hertzberg, "Experimental uncertainties associated with particle image velocimetry (PIV) based vorticity algorithms," *Experim. Fluids*, vol. 26, no. 1, pp. 36–54, Jan. 1999.
[31] M. Markl, A. Frydrychowicz, S. Kozerke, M. Hope, and O. Wieben, "4D flow MRI," *J. Magn. Reson. Imag.*, vol. 36, no. 5, pp. 1015–1036, Nov. 2012.
[32] G. Haller, "An objective definition of a vortex," *J. Fluid Mech.*, vol. 525, pp. 1–26, Feb. 2005.
[33] P. E. Shrout and J. L. Fleiss, "Intraclass correlations: Uses in assessing rater reliability," *Psychol. Bull.*, vol. 86, no. 2, pp. 420–428, Mar. 1979.
[34] E. K. Kerut, "The mitral L-wave: A relatively common but ignored useful finding," *Echocardiography*, vol. 25, no. 5, pp. 548–550, May 2008.
[35] L. P. Badano *et al.*, "Current clinical applications of transthoracic three-dimensional echocardiography," *J. Cardiovascular Ultrasound*, vol. 20, no. 1, pp. 1–22, 2012.
[36] P. P. Sengupta, G. Pedrizetti, and J. Narula, "Multiplanar visualization of blood flow using echocardiographic particle imaging velocimetry," *JACC Cardiovascular Imag.*, vol. 5, no. 5, pp. 566–569, May 2012.
[37] A. Gomez *et al.*, "4D blood flow reconstruction over the entire ventricle from wall motion and blood velocity derived from ultrasound data," *IEEE Trans. Med. Imag.*, vol. 34, no. 11, pp. 2298–2308, Nov. 2015.
[38] J. Provost *et al.*, "3D ultrafast ultrasound imaging *in vivo*," *Phys. Med. Biol.*, vol. 59, no. 19, pp. L1–L13, 2014.
[39] W. F. Walker and G. E. Trahey, "A fundamental limit on delay estimation using partially correlated speckle signals," *IEEE Trans. Ultrason., Ferroelect., Freq. Control*, vol. 42, no. 2, pp. 301–308, Mar. 1995.
[40] P. Song, A. Manduca, J. Trzasko, and S. Chen, "Ultrasound small vessel imaging with block-wise adaptive local clutter filtering," *IEEE Trans. Med. Imag.*, to be published, doi: 10.1109/TMI.2016.2605819.
[41] L. Tong, A. Ramalli, R. Jasaityte, P. Tortoli, and J. D'hooge, "Multi-transmit beam forming for fast cardiac imaging—Experimental validation and *in vivo* application," *IEEE Trans. Med. Imag.*, vol. 33, no. 6, pp. 1205–1219, Jun. 2014.

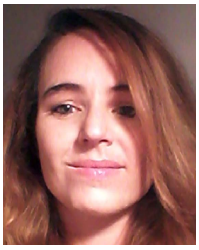

Julia Faurie received the B.Sc. degree in computer science from the University Paris 12, Créteil, France, in 2000, and the master's degree in imaging sciences from the University Pierre et Marie Curie, Paris, in 2002. She is currently pursuing the Ph.D. degree in biomedical engineering with the University of Montreal.

Her current research interests, performed at the Research Unit of Biomechanics & Imaging in Cardiology, University of Montreal Hospital Research Center, include cardiac and flow ultrasound imaging.

Mathilde Baudet received the Medical Degree in cardiology and the master's degree in cellular biology, physiology and pathology of cardiovascular system from the University of Paris VII, Paris, France, in 2013.

She is a Postdoctoral Fellow with the Department of Echocardiography, University of Montreal Hospital (CHUM), Canada. Her current research interests include cardiac ultrasound and magnetic resonance imaging.

Kondo Claude Assi received the M.Sc. degree in applied mathematics and the Ph.D. degree in computer engineering from the École Polytechnique of Montreal, QC, Canada, in 2008 and 2014, respectively.

He was with the Imaging and 4D Vision Laboratory (LIV4D), Department of Computer Engineering, École Polytechnique of Montréal, and the Non-Invasive Active Vision Orthopedics Laboratory (LAVIANI), Sainte-Justine Hospital Research Center of Montréal. He joined the RUBIC unit, University of Montréal Hospital Research Centre, Montréal, in 2015 as a Postdoctoral Fellow. His current research interests include vector flow imaging by ultrasound imaging.

Dominique Auger completed her training in cardiology at the University of Montréal in 2009. She received the Ph.D. degree in cardiac imaging in heart failure from Leiden University in 2014.

Her work focuses on heart failure, cardiac magnetic resonance imaging, and echocardiography.

Guillaume Gilbert received the B.Sc. and Ph.D. degrees in physics from the University of Montréal, Montréal, QC, Canada, in 2005 and 2009, respectively.

He is currently MR Clinical Scientist for Philips Healthcare Canada and Associate Professor with the Department of Radiology, Radio-Oncology and Nuclear Medicine, University of Montréal. His current research is centered around magnetic resonance imaging (MRI) methodology, with a special interest towards neuro, abdominal, and cardiovascular imaging.

François Tournoux received the M.D. degree from the French University of Paris 5 and the Ph.D. degree from the French University of Paris 7. He completed his clinical training at the Hôpital Lariboisière and Hôpital Bichat, Paris, France, and his research training at the Massachusetts General Hospital, Boston, MA, USA.

He is a member of the CHUM department of cardiology, an Adjunct Clinical Professor with the University of Montréal, and a clinician researcher at the echocardiography laboratory. He specializes in non-invasive cardiac imaging, cardiac insufficiency, and sports cardiology. These subspecialties are also its main areas of research.

Damien Garcia received the Engineering degree in mechanical engineering from the École Centrale de Marseille, France, in 1997, and the Ph.D. degree in biomedical engineering from the University of Montréal, QC, Canada, in 2003.

He was a Postdoctoral Fellow with the Department of Echocardiography, Gregorio Marañón Hospital, Madrid, Spain, from 2006 to 2008. He is currently the Director of the Research Unit of Biomechanics & Imaging in Cardiology, University of Montréal Hospital Research Center, and an Associate Professor with the Department of Radiology, Radio-Oncology and Nuclear Medicine, University of Montréal. His current research interests include cardiac/cardiovascular ultrasound imaging, mostly in fluid dynamics and flow imaging (www.biomecardio.com).

Dr. Garcia is an Associate Editor of IEEE TRANSACTIONS ON ULTRASONICS, FERROELECTRICS, AND FREQUENCY CONTROL. He serves on the Technical Program Committee of the IEEE Ultrasonics Symposium.